

# MULTIBODY MODEL OF FLYING WING WITH SIGNIFICANT DEFORMATION

Balazs GATI, PhD\*

\*Budapest University of Technology and Economics  
Department of Aircraft and Ships

**Keywords:** *elastic, multibody, vortex-lattice, flying wing, UAV*

## Abstract

*The mishap of the Helios has shown that the control of the high-wingspan flying wing is not properly solved as of today. The reason is the significant deformation that cannot be described by the conventional single body models.*

*The model presented in this paper treats wings with high aspect ratio as a chain of flying bodies. The lift distribution over the wing is calculated using a built-in Vortex-Lattice method in every step of the simulation.*

## 1 Prelude

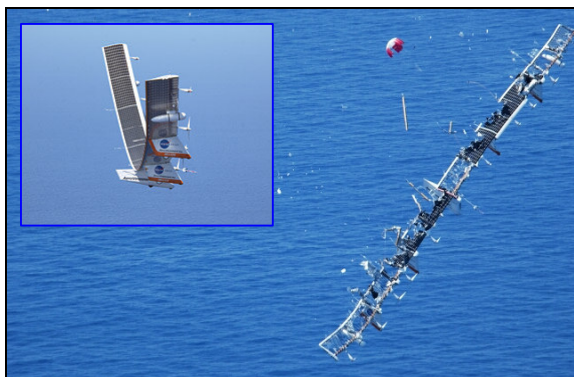


**Fig. 1. Helios in flight and immediately before impact**

After a research period of 20 years, the NASA and the AeroVironment, Inc. has constructed the fifth-generation HALE (High Altitude Long Endurance) UAV called the Helios. The wingspan of the aircraft was 247 ft, and it had an aspect ratio of about 30. The high aspect ratio, however, did not result in a heavy structure by the flying wings, because the distributed lift could counteract to the distributed weight optimally, and thus the

bending moment in the wingspar is significantly less than in conventional wing-and-fuselage structures.

The Helios took off for the last flight on June 26, 2003. The reason of the mishap was an unexpectedly high degree of pitch instability by high wing dihedral, which led to a high-speed dive and loss of wing skin due to the high dynamic pressure. The primary structure of the wing was intact up until the impact in the ocean.

The investigation report [1] established that the primary cause of the mishap was the insufficient knowledge about the behavior of the aircraft by high dihedral.

## 2 Modeling of Flying Wings with Significant Deformation

On the video footage showing the Helios' previous successful flights, one can observe that the wing does not really behave as a classic elastic body. If some disturbance deforms the wing, the structure has not enough elasticity to force it back into the original shape. Thus the behavior of the wing looks more likely flexible than elastic, especially in the case of dihedral deformation.

Based on this observation, we create a model to simulate the motion and deformation of the near-flexible or even fully flexible flying wings. In this case, the multibody approach appeared the best choice, where the elastic forces have minimal or negligible role compared to the mass forces.

A flexible flying wing is unserviceable without affordable flight and deformation control. Constructing the above-mentioned model is the first step to develop control that

can provide “virtual stiffness” for the wing, and supersedes the heavy wingspar. Thus, we can get a flying object with significantly improved payload/take-off-weight ratio, which is a critical parameter with HALE UAV-s because of the power consumption.

## 2.1 The Multibody Model

A multibody model consists of bodies and the connections between them. A very simple multibody system is a hang-glider [2], consisting of two bodies: the pilot and the wing.

In the case of Helios-like flying wings, the first step to create a multibody model is to partition the wing into smaller bodies, which requires more consideration than hang-gliders. Flying wings always have a high aspect ratio, and thus the deformation of the wing sections is negligible compared to the wing dihedral and wing twist. Therefore, we have split the wing in spanwise direction only (Fig. 2).

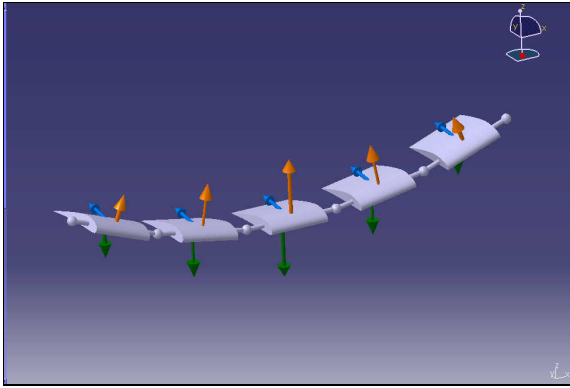


Fig. 2. Splitting the wing into bodies

The second step is to define the connections. (Fig. 3.) We have chosen one ball joint between each body, which enables the relative rotation but blocks the relative displacement of the adjacent bodies. Each direction of the rotation can be affected by a cylindrical spring and a damper with different parameters as well, similarly to the different stiffness and structural damping of the wing in the three directions.

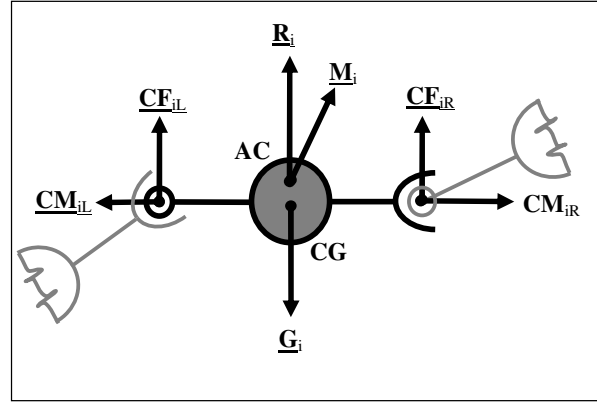


Fig. 3. Kinetic scheme

The equations (1) and (2) describe the motion of a single body of the multibody system:

$$m_i \cdot [\dot{V}_i + \Omega_i \times V_i] = \begin{aligned} &= \underline{M}_{iG} \cdot \underline{G}_i + \underline{M}_{iAi} \cdot \underline{R}_i - \underline{M}_{iG} \cdot \underline{M}_{GL} \cdot \underline{L} \cdot \underline{CF}_{iL} \\ &+ \underline{CF}_{iR} \end{aligned} \quad (1)$$

$$\begin{aligned} \underline{I}_{i} \cdot \dot{\Omega}_i + \Omega_i \times \underline{I}_{i} \cdot \Omega_i = & \\ &= -\underline{r}_{iCL} \times \underline{M}_{iG} \cdot \underline{M}_{GL} \cdot \underline{L} \cdot \underline{CF}_{iL} + \\ &+ \underline{r}_{iCR} \times \underline{CF}_{iR} - \underline{M}_{iG} \cdot \underline{M}_{GL} \cdot \underline{L} \cdot \underline{CM}_{iL} \\ &+ \underline{CM}_{iR} + \underline{r}_{iACi} \times (\underline{M}_{iAi} \cdot \underline{R}_i) + \underline{M}_i \end{aligned} \quad (2)$$

$$\begin{aligned} \underline{M}_{Gi} \cdot [\dot{V}_i + \Omega_i \times V_i + \dot{\Omega}_i \times \underline{L}_{iCG} + \Omega_i \times (\Omega_i \times \underline{L}_{iCG})] = & \\ = \underline{M}_{GHi} \cdot [\dot{V}_{i+1} + \Omega_{i+1} \times V_{i+1} + \dot{\Omega}_{i+1} \times \underline{L}_{i+1Ci} + \Omega_{i+1} \times (\Omega_{i+1} \times \underline{L}_{i+1G})] \end{aligned} \quad (3)$$

The left side of the equation (3) calculates the acceleration of the connection point based on the motion of the left body, while the right side calculates the same, but based on the right body. The equation reflects that the two accelerations must be equal, i.e. the bodies must remain connected at the connection point. The force emerging in the connection point is one of the variables of the equation system, and will be calculated during the solving procedure.

Based on the above-mentioned three equations, the motion of a flying chain can be simulated. If we wish to give some elastic behavior to the model, we can use, for example,

equation (4) to provide for moment and structural damping in the connection point. The  $\psi_{i,i+1}, \vartheta_{i,i+1}, \phi_{i,i+1}$  are the Euler-angles between the adjacent bodies.

$$\underline{CM}_{i,i+1} = \begin{bmatrix} k_1 \cdot \psi_{i,i+1} \\ k_2 \cdot \vartheta_{i,i+1} \\ k_3 \cdot \phi_{i,i+1} \end{bmatrix} + \begin{bmatrix} k_4 \cdot \dot{\psi}_{i,i+1} \\ k_5 \cdot \dot{\vartheta}_{i,i+1} \\ k_6 \cdot \dot{\phi}_{i,i+1} \end{bmatrix} \quad (4)$$

In the next step, the equations can be transposed in order to build the following type of equation system:

$$\underline{A}\dot{\underline{x}} = \underline{b}(\underline{x}, \underline{u}(t)) \quad (5)$$

This type of equation system can be solved by means of numerical methods, namely the multiplication of the numerically calculated  $\underline{A}^{-1}$  (which is equal to the inverse of the  $\underline{A}$  matrix) and the right side results in the  $\dot{\underline{x}}$  vector. The numerical integration provides the values of the  $\underline{x}$  vector in the function of time, which, once evaluated, can predict the behavior of this type of flying object.

## 2.2 Aerodynamics Based on the Vortex-Lattice Method

The lift distribution over the wing is calculated by means of the Vortex-Lattice method based on [3] and [5]. To keep the calculation time low, the vortices in the fixed wake do not change their position.

The drag is calculated by means of the Blasius-equation with increasing Re number along the chord.

## 2.3 Trim calculation

The trim calculation is based on the general assumption that the derivatives of the variables are zero in stationary flight. This means that the left side of equation system (5) is zero. The Newton-Raphson method can find values for the  $\underline{x}$  vector, which causes the  $\underline{b}$  vector to be equal to zero. It is not necessary to determine the value of every variable because some of them are naturally zero in trimmed flight.

## 2.4 The Software

The simulation software was written in the MATLAB language. The preprocessor calculates the parameters of each body in the system, based on the pre-defined parameters of the entire wing.

The integration is performed by MATLAB's built-in solver that is based on the explicit Runge-Kutta (4,5) formula, namely, the Dormand-Prince pair. The  $\underline{A}$  matrix in (5) is calculated automatically for any number of bodies in the multibody model. The values of  $\underline{A}^T$  are recalculated by means of a Gaussian elimination with partial pivoting in every time step, in order to take into account the non-linearities in the model.

The postprocessor first checks if the bodies would noticeably disconnect as a result of the numerical integration inaccuracy, then calculates the time function of the parameters involved in the analysis.

The visualization module of the software plots figures, diagrams and 3D graphs to support the analysis.

## 3 Analysis of the Model and the Simulation

The model and the simulation has been available for less than a year, and considerable investigation is necessary to evaluate such complex models and calculations, therefore the work is still in progress.

The first investigations concentrated on the flight-mechanical and the numerical side of the model. To keep the complexity of the simulation low, these evaluations omitted the Vortex-Lattice method and used simple aerodynamic parameters to calculate the lift, drag and momentum generated by the wing. In this phase of the evaluation, a low CG flying wing configuration was created, consisting of five bodies, which seems an affordable choice for the future investigation of the Vortex-Lattice method as well. The advantage of this configuration is the natural longitudinal stability, which supersedes a built-in control system and/or a special S-chord profile whose special behavior would increase the complexity of the evaluation. On the other hand, the five

bodies are enough to observe complex deformations but keep the computational effort low.

The results of the first investigation phase showed success, and subsequently, we incorporated the Vortex-Lattice method into our model. The new feature significantly extended the simulation time, so we had to work with 72 grid points to keep the simulation time below one hour on a 2.6 GHz Pentium 4 computer. This was not a serious problem because at this stage of the project, we tested the model only, thus the precision of the simulation was not the most important aspect of the evaluation.

### 3.1 Numerical Investigation

In the numerical methods used by the simulation, we tested how the changing of four parameters affect the processor time and the outcome of the simulation. At first, we had to find an affordable value for the damping coefficient in the Newton-Raphson method. As a result, we are using the value  $k_{NR}=2^2$  if we can start it near the trim condition. However, if we are unable to predict it precisely, we have to use a value as big as  $k_{NR}=2^{10}$ , especially if the stiffness of the wing is defined at a significantly lower value than that of a rigid one. Of course, this value affected the computational demand only, not the precision of the trim condition.

However, changing the tolerance of the Newton-Raphson method changed the outcome of the simulation. Based on Fig. 4., we chose the value of  $10^{-4}$  as a balance between processor time and precision, because the value of  $10^{-6}$  did not significantly improve the result of the simulation.

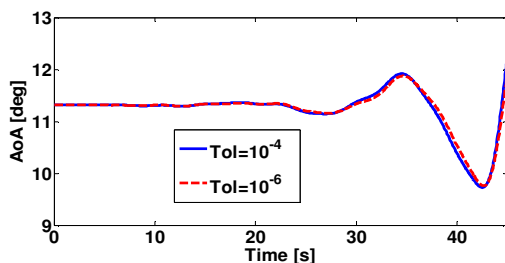


Fig. 4. Sensitivity of AoA on the tolerance of the Newton Raphson method

We looked for the affordable value of the tolerance of the Runge-Kutta solver, too. The effect of the tolerance was only remarkable in the disconnect checking between the bodies. We have chosen a value of  $10^{-4}$  to keep the cumulated separation lower than  $10^{-5}$  m.

The simulation of stationary flights always resulted in a divergent lateral oscillation started about by  $t=10s$ . We carried out the same 50s stationary flight simulation, this time with 264 grid points, in order to investigate how the number of gridpoints affect the outcome of the simulation. The calculation ran for 21 hours. shows the difference.

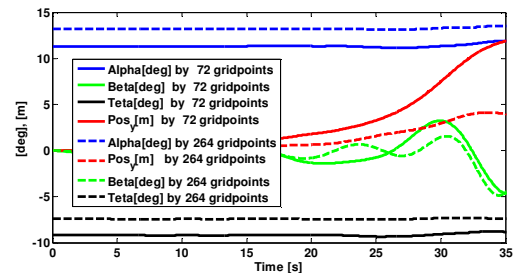


Fig. 5. Effect of No. of gridpoints on the simulation

The red curves represent the lateral displacement of the middle body; the dashed ones show the result of the improved simulation. The simulation with the higher number of grid points shows three times less lateral displacement after 35s.

### 3.2 The Flight-mechanical Investigation

The Fig. 6 presents two simulations, the left one with lighter middle body than the right one.

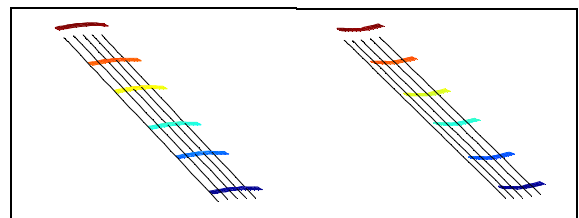


Fig. 6. Flight path and wing shape by different weight distributions

The wing dihedral looks to give appropriate answer on the change in the weight distribution.



The simulation of wing twist caused by elevon deflection was an other qualitative test. The resulted shape can be observed in Fig. 7. The calculated deformation suits the expectations.

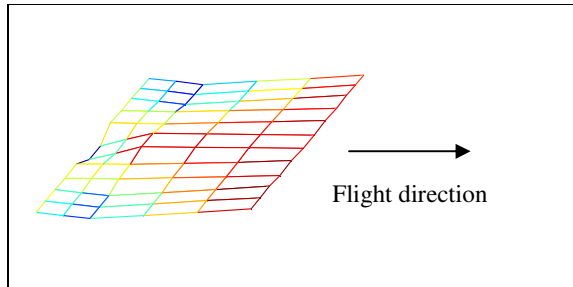


Fig. 7. Effect of outer elevon deflection on wing shape

### 3.3 Radio-controlled Test Model

The next step is the validation of the model that means comparing the results of the simulation to real test flights. A year ago, we started the Open Airborne Test Platform project to find affordable technology to construct low-cost RC models in a limited time, for different kinds of test flights. So far, we have built three RC models. The first one (Fig. 8) has a conventional configuration with an unusual elastic wing in order to test elastic materials and technology.



Fig. 8. RC model with elastic wing

The second one is a conventional training plane, which, at the same time, serves as testbed

for measurement and control systems. The first time we applied the initial experience acquired from the multibody model was when we designed [6] the third RC model. The specialty of this plane is the active aeroelastic control around the length axis (Fig. 9)



Fig. 9. RC model with active aeroelastic aileron control and onboard camera

The fourth RC model (Fig. 10) is under construction. It is designed to validate the multibody model of near flexible flying wings, described above.

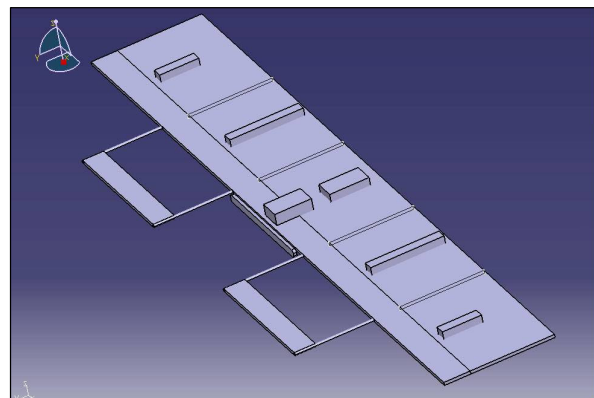


Fig. 10. 3D view of the RC model designed to validate the multibody model

### 4 Future Work

We expect to finish the validation of the model in the near future: then it will be ready to apply

in the design of the next generation HALE UAV or similar flying objects. The key point of the development is an advanced control system, which can be designed and tested on the basis of our model.

In the long run, our model is able to describe the behavior of a system of autonomous UAVs as well, where the units are connected to each other and form a large wingspan flying chain, in order to utilize the advantage of distributed weight, distributed lift, distributed trust and minimal induced drag.

## References

- [1] Noll T. E., Brown J. M., Perez-Davis M. E., Ishmael S. D., Tiffany G. C. and Gaier M. *Investigation of the Helios Prototype Aircraft Mishape*. 2004
- [2] Gati B. *Investigation of Flight Dynamic of Hang-glider* Acta Polytechnica, Journal of Advanced Engineering Design ISSN 1210-2709, Vol.40 No.1/2000 pp.3-6, Prague, 2000. January,
- [3] Shabana A. A., *Dynamics of Multibody Systems*, "A Wiley-Interscience publication", 1989, ISBN 0-471-61494-7
- [4] Katz J. and Plotkin A. *Low-speed aerodynamics* McGraw-Hill, Inc., 1991
- [5] Somos M. *Repülőgépszárnyak viselkedésének vizsgálata időben változó megfűvés esetén, ideális áramlásban* Diploma thesis, BUTE Dept. of Aircraft and Ships, 2005, Budapest
- [6] Szokol R. *Aktiv aeroelasztikus csűrőkormányzás lehetőségének vizsgálata* Diploma thesis, BUTE Dept. of Aircraft and Ships, 2006, Budapest